

Experiments in Robot Control from Uncalibrated Overhead Imagery

Rahul Rao¹, Camillo Taylor¹, and Vijay Kumar¹

GRASP Laboratory, University of Pennsylvania
(rahulrao, cjtaylor, kumar)@grasp.cis.upenn.edu
<http://www.grasp.upenn.edu>

Abstract. In this work we address the problem of controlling a ground robot based on aerial image feedback in real time. We present an analysis of the relationship between a robot's ground velocity and the velocity of its projection in the image. We also show how a subset of the parameters of the homography relating the ground plane and the image plane can be extracted from motion correspondences and subsequently used in a sample control task. Further, we extend our analysis to the case of robot control from a moving overhead camera using image feedback. The experimental implementation and validation of the schemes we have presented is one of the central goals of this paper.

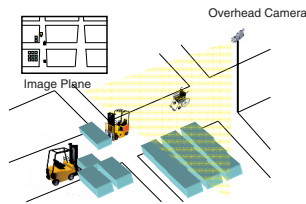


Fig. 1. Control of Vehicles in a Warehouse Using an Overhead Camera

1 Introduction

We are interested in applications in automation and robotics where overhead cameras can provide information that can be used to guide mobile robots. In a factory, a network of overhead cameras can be used to sense positions of robots, guide them around obstacles, and coordinate their motions toward their destinations. Outdoors, aerial vehicles with cameras can be used to guide ground vehicles toward targets. In the first example, it is possible to calibrate overhead cameras and instrument the robots and the environment. However, in general, we would like to be able to consider an *ad-hoc* network of uncalibrated cameras in an unstructured environment. This is particularly relevant for field robotics where the aerial vehicle's position and orientation will change over time, and it is difficult to instrument and structure the outdoor environment.

The goal of our research is to develop a theoretical formulation as well as a real time implementation scheme for the control of an unmanned ground vehicle (UGV) from an unmanned aerial vehicle (UAV) or an overhead camera. A simple

situation where such an approach to automation will be useful is shown in Figure 1 which shows forklifts transporting objects in a warehouse while being monitored by an overhead camera. Such an approach can enable the use of personal robots in unstructured environments and AGVs and automated fork-lifts on factory floors without structuring or instrumenting the environment with landmarks, beacons or radio tags.

It is natural to ask what the motivation for such a *distributed sensing system* is. Such a configuration offers some advantages over onboard sensing. An onboard sensing system has *line of sight* sensing only and will thus rely on partial path planning strategies that will need to be updated on a regular basis in order to get the robot from its current position to a desired final position. Further, data fusion over space and time can be done effectively using distributed sensing. For example, if another camera were added to the existing system in Figure 1, the two cameras could be networked in order to provide a wider view of the environment as compared to a single overhead camera or a single onboard camera.

Our goal is the development of motion planning strategies and control of ground robots using feedback from a single, uncalibrated, overhead camera. The intention is to transfer the control problem from the real world to the image plane. Once the control problem is solved in the image plane there is a need to relate these quantities to control quantities (typically translational and angular velocities) used to guide the robot on the ground. In this paper we present a novel analysis of the relationship between the ground velocity of a vehicle and the velocity of its projection in the image. This is particularly useful in situations where robot velocity needs to be regulated, as mentioned above. We present in this work a metric relationship between image plane and ground plane velocities obtained by motion correspondences.

This paper is organized as follows- Section 2 presents an overview of related research in the use of visual feedback for control tasks. Section 3 presents an analysis and the metric relationship between the robot velocity on the ground plane and the velocity of it's projection in the image plane. Section 4 presents the use of the calibration procedure described in Section 3 to control the point to point motion of a robot from image feedback. Section 5 presents experimental validation of the ideas presented previously, followed by some concluding remarks in Section 6.

2 Previous Research

Robust feedback control schemes have been proposed ([1], [4], [5]) that are capable of accurately regulating a system to a desired configuration even when parameters relating the two frames are not exactly known [3]. Overhead imagery has been used in the past where the relationships between the two frames is *a priori* known. It has also been used in the situation where the image plane is parallel to the ground plane [2], thereby reducing the problem to finding a similarity transformation (4 parameters) relating the two planes rather than the more general projective transformation (8 parameters). Our work is novel in the sense that no knowledge is assumed of the intrinsic parameters of the camera or about the relative pose of the image plane with respect to the ground plane.

As far as robot manipulation tasks are concerned, research in visual servoing has been classified broadly into one of two approaches—*position based* and *image based* control systems [11]. In a *position based* (or *3D visual servoing*) control system features are extracted from the image and used in conjunction with a geometric model of the target and the known camera model to estimate the target's pose with respect to the camera. Control inputs are computed based on the errors in the estimated pose space thus making camera calibration necessary for reliable control. In the *image based* (or *2D visual servoing*) approach, controls are computed directly on the basis of image features, thus reducing errors due to sensor modeling and camera calibration. Taking advantage of *2D* and *3D* visual servoing techniques is the approach called *2-1/2 D* visual servoing. This approach is claimed to be more robust with respect to calibration errors, though it is also more sensitive to image noise if image features are used to compute control inputs [12].

In contrast to the papers mentioned above which mostly deal with kinematic models, visual feedback can also be combined with systems with second order dynamics. Ma, Košečka and Sastry [9] used visual servoing techniques to control the motion of a car based on information obtained from a camera mounted on the vehicle. Zhang and Ostrowski [8] used visual servoing techniques for the control of an unmanned blimp. Cowan and Koditschek [13] used navigation functions on the image plane to design image-based servo algorithms to guide a planar convex rigid body to a static goal for all initial conditions within the camera's workspace. Current efforts [14] explore air-ground collaboration for feature localization with the air and ground vehicles complementing each others observations and sensor platform characteristics.

3 Relating the Robot's Ground and Image Plane Velocities

In this section we investigate the relationship between a vehicles velocity on the ground plane and the velocity of its projection in a fixed overhead camera. We will assume some means for measuring the velocity of the ground vehicle with respect to a fixed frame. For example, an unmanned ground vehicle equipped with a compass and an odometry system would be able to measure it's heading and speed with respect to a fixed magnetic reference frame. We expect, however, that these velocity measurements will contain errors which make it impractical to deduce the displacement of the robot by integrating velocity readings over time.

We perceive a situation where an overhead camera has sight of a ground robot and the desired trajectory. Let $\mathbf{w} \equiv (x, y, 1)^T$ denote the homogeneous coordinates of a point on the ground plane and $\mathbf{c} = (u, v, 1)^T$ denote the coordinates of the projection of \mathbf{w} in the image. It is easy to show that \mathbf{w} and \mathbf{c} are related by a projective transformation \mathbf{G} . This can be expressed as

$$\mathbf{c} \propto \mathbf{G}\mathbf{w}, \quad \mathbf{G} \in GL(3) \quad (1)$$

$$\Rightarrow \mathbf{w} \propto \mathbf{H}\mathbf{c} \quad (2)$$

where $\mathbf{H} = \mathbf{G}^{-1}$.

For clarity, the matrices \mathbf{G} and \mathbf{H} be represented in terms of their columns as $\mathbf{G} = (G^1 \ G^2 \ G^3)$ and $\mathbf{H} = (H^1 \ H^2 \ H^3)$ respectively. Similarly, they can be represented in terms of their rows as $(G_1 \ G_2 \ G_3)^T$ and $(H_1 \ H_2 \ H_3)^T$ respectively. Note that superscripts and subscripts are used to distinguish between matrix columns and rows. Replacing the proportionality sign in (2) by an equality we get

$$\mathbf{w} = \lambda \mathbf{Hc} \tag{3}$$

where $\lambda = \frac{1}{H_3 \cdot \mathbf{c}}$. Similarly, the image coordinates, $(u \ v)$, can be expressed in terms of the homogeneous ground plane coordinates, \mathbf{w} , as follows:

$$u = \frac{G_1 \cdot \mathbf{w}}{G_3 \cdot \mathbf{w}} \quad (4), \quad v = \frac{G_2 \cdot \mathbf{w}}{G_3 \cdot \mathbf{w}} \quad (5)$$

Differentiating (4) with respect to time yields

$$\dot{u} = \frac{(G_3 \cdot \mathbf{w})(G_1 \cdot \dot{\mathbf{w}}) - (G_1 \cdot \mathbf{w})(G_3 \cdot \dot{\mathbf{w}})}{(G_3 \cdot \mathbf{w})^2} \tag{6}$$

Using the expression for \mathbf{w} from (3) we get

$$\dot{u} = \frac{(G_3 \cdot (\lambda \mathbf{Hc}))(G_1 \cdot \dot{\mathbf{w}}) - (G_1 \cdot (\lambda \mathbf{Hc}))(G_3 \cdot \dot{\mathbf{w}})}{(G_3 \cdot (\lambda \mathbf{Hc}))^2} \tag{7}$$

Also, $G \cdot H = I$.

Using these facts, and the expression for λ , we can simplify (7) to yield

$$\dot{u} = (H_3 \cdot \mathbf{c})[G_1 \cdot \dot{\mathbf{w}} - u(G_3 \cdot \dot{\mathbf{w}})] \tag{8}$$

$$\dot{v} = (H_3 \cdot \mathbf{c})[G_2 \cdot \dot{\mathbf{w}} - v(G_3 \cdot \dot{\mathbf{w}})] \tag{9}$$

These expressions can be written compactly as

$$\begin{pmatrix} \dot{u} \\ \dot{v} \end{pmatrix} = (H_3 \cdot \mathbf{c}) \begin{pmatrix} G_1 \cdot \dot{\mathbf{w}} - u(G_3 \cdot \dot{\mathbf{w}}) \\ G_2 \cdot \dot{\mathbf{w}} - v(G_3 \cdot \dot{\mathbf{w}}) \end{pmatrix} = (H_3 \cdot \mathbf{c}) \begin{pmatrix} 1 & 0 & -u \\ 0 & 1 & -v \end{pmatrix} \mathbf{G} \dot{\mathbf{w}} \tag{10}$$

where $\dot{\mathbf{w}} = (\dot{x}, \dot{y}, 0)^T$. This can be rewritten as

$$\begin{pmatrix} \dot{u} \\ \dot{v} \end{pmatrix} = (H_3 \cdot \mathbf{c}) \begin{pmatrix} 1 & 0 & -u \\ 0 & 1 & -v \end{pmatrix} (G^1 \ G^2) \begin{pmatrix} \dot{x} \\ \dot{y} \end{pmatrix} \tag{11}$$

Note that H_3 , the third row of \mathbf{H} , can be expressed in terms of the columns of \mathbf{G} as

$$H_3 = \frac{G^1 \times G^2}{(G^3) \cdot (G^1 \times G^2)} = \frac{G^1 \times G^2}{\det(\mathbf{G})} \tag{12}$$

Since the matrix \mathbf{G} represents a projective transformation, it's scale is immaterial which means that we can, without loss of generality, restrict \mathbf{G} to be a matrix with

unit determinant. Alternatively, one can note that scaling the matrix \mathbf{G} by a constant does not affect equation (11). With this restriction, equation (11) becomes:

$$\begin{pmatrix} \dot{u} \\ \dot{v} \end{pmatrix} = ((G^1 \times G^2) \cdot \mathbf{c}) \begin{pmatrix} 1 & 0 & -u \\ 0 & 1 & -v \end{pmatrix} (G^1 \ G^2) \begin{pmatrix} \dot{x} \\ \dot{y} \end{pmatrix} \quad (13)$$

This equation has a number of notable features. It provides a metric relationship between the velocity of the robot on the ground plane (\dot{x}, \dot{y}) and the velocity of its projection in the image (\dot{u}, \dot{v}) . Strangely, it does this without requiring a normalizing division such as the ones implied by the projective relationships given in Equations (1) and (2). The expression reveals that the observed image velocity depends linearly on the ground plane velocity, (\dot{x}, \dot{y}) , and quadratically on the vectors G^1 , G^2 and \mathbf{c} .

Note that this expression only involves the first two columns of \mathbf{G} which means that we cannot recover information about the third column of \mathbf{G} solely from measurements of vehicle and image velocities. We can only hope to recover information about 6 of the 8 degrees of freedom that define the homography \mathbf{G} . The missing two degrees of freedom can be accounted for by noting that the origin of the ground planes reference frame can be chosen arbitrarily.

3.1 Camera Calibration from Motion Correspondences

We can recover the vectors G^1 and G^2 from image measurements by observing that the right hand side of equation (11) must be perpendicular to the vector $(-\dot{v} \ \dot{u})$. This translates to:

$$(-\dot{v} \ \dot{u}) \cdot \begin{pmatrix} 1 & 0 & -u \\ 0 & 1 & -v \end{pmatrix} (G^1 \ G^2) \begin{pmatrix} \dot{x} \\ \dot{y} \end{pmatrix} = 0 \quad (14)$$

This homogeneous equation is linear in the unknown vectors G^1 and G^2 . Given five separate measurements of a vehicles position in the image (u, v) , it's instantaneous image velocity, (\dot{u}, \dot{v}) , and its ground plane velocity, (\dot{x}, \dot{y}) , we can construct a system of linear homogeneous equations which allows us to recover G^1 and G^2 up to an unknown scale factor, that is $(G^1 \ G^2) = \alpha (\hat{G}^1 \ \hat{G}^2)$. This scale parameter, α , can be resolved by substituting the scaled versions of G^1 and G^2 into equation (13) and enforcing equality as follows:

$$\begin{pmatrix} \dot{u} \\ \dot{v} \end{pmatrix} = \alpha^3 ((\hat{G}^1 \times \hat{G}^2) \cdot \mathbf{c}) \begin{pmatrix} 1 & 0 & -u \\ 0 & 1 & -v \end{pmatrix} (\hat{G}^1 \ \hat{G}^2) \begin{pmatrix} \dot{x} \\ \dot{y} \end{pmatrix} \quad (15)$$

4 An Image Based Feedback Linearizing Controller

We now describe a simple feedback linearizing controller that is built in the image plane and enables the robot to navigate from a certain starting state in the image to a desired destination, also in the image. Under the assumption that the motion of the robot is limited to a plane, this translates to motion from a starting point in the

real to a desired destination in the real world. However, building the controller in the image plane makes it possible to do so without any real time knowledge or feedback of the position of the robot in the real world (i.e. (x, y)). All we need to know is the position of the robot in the image (i.e. (u, v)) and its orientation relative to a starting orientation, and that enables us to build such a controller. The controller has been experimentally tested in real time along with the calibration system that has been outlined in Section 3.1. Details of the experiments are presented in Section 5.2.

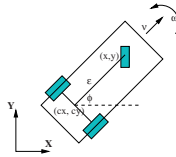


Fig. 2. A representation of the robot model used for image- based control tasks.

Let (u, v) be the image coordinates of a point (x, y) that lies a distance ϵ off the center of the rear axle, (c_x, c_y) , of the robot, as shown in Figure 2. This means

$$\begin{aligned} x &= c_x + \epsilon \cos \phi \\ y &= c_y + \epsilon \sin \phi \end{aligned} \tag{16}$$

From equation (11), we obtain

$$\begin{pmatrix} \dot{u} \\ \dot{v} \end{pmatrix} = (H_3 \cdot \mathbf{c}) \begin{pmatrix} 1 & 0 & -u \\ 0 & 1 & -v \end{pmatrix} (G^1 \ G^2) \begin{pmatrix} \dot{x} \\ \dot{y} \end{pmatrix} \tag{17}$$

$$= \mathbf{J} \begin{pmatrix} \dot{x} \\ \dot{y} \end{pmatrix} \tag{18}$$

Differentiating equation (16) once yields

$$\begin{pmatrix} \dot{x} \\ \dot{y} \end{pmatrix} = \begin{pmatrix} \cos \phi & -\epsilon \sin \phi \\ \sin \phi & \epsilon \cos \phi \end{pmatrix} \begin{pmatrix} \nu \\ \omega \end{pmatrix} = \mathbf{ZV} \tag{19}$$

where $\mathbf{V} = (\nu, \omega)$ represents the forward and angular speeds of the robot respectively. Thus

$$\begin{pmatrix} \dot{u} \\ \dot{v} \end{pmatrix} = \mathbf{JZV} \tag{20}$$

Now, if we desire to move the robot to the desired image coordinates given by (u^D, v^D) , then we can choose, as a simple example, a proportional feedback controller of the type

$$\begin{pmatrix} \dot{u} \\ \dot{v} \end{pmatrix} = -\mathbf{K} \begin{pmatrix} u - u^D \\ v - v^D \end{pmatrix} \tag{21}$$

\mathbf{K} being a gain matrix with appropriately chosen gains. Thus the desired controls that need to be applied to the robot to get it to its desired position in the image can be obtained as

$$\mathbf{V}^D = -(\mathbf{JZ})^{-1}\mathbf{K} \begin{pmatrix} u - u^D \\ v - v^D \end{pmatrix} \quad (22)$$

We note here that since we have chosen a reference point that is not on the center of the axle (i.e. $\epsilon \neq 0$), the inverse of the matrix represented above always exists and there are no singularities.

5 Experimental Results

In order to investigate the efficacy as well as the feasibility of the proposed technique experiments were performed with an actual robotic platform. The experimental tasks involved extracting a subset of the parameters of the homography using the methods presented in the previous sections followed by the motion of the robot to a desired destination chosen in the camera image, in real time. Further, the overhead camera was subjected to random disturbances to observe the performance of the simple image stabilization technique using fixed fiducials on the ground plane that were tracked continuously during the robot's motion.

As has been outlined in Section 3.1 the vectors G^1 and G^2 can be recovered from at least five distinct measurements of $(u, v, \dot{u}, \dot{v}, \dot{x}, \dot{y})$ as the robot moves on the ground. Our tests gave us an idea of the accuracy of the results returned by our online estimation procedure.

5.1 Camera Calibration from Motion Correspondences

We conducted a series of experiments with the ER-1 mobile robot from Evolution Robotics and an overhead Dragonfly firewire camera with a Sony ICX204 sensor. The ER-1 is a three-wheeled, Hilare-like robot and is shown in Figure 3.

As mentioned in Section 3.1, the robot was moved in increments of 30° for 8 segments. The path of the robot along with a camera view of the robot as it moves during calibration are shown in Figure 3. It was continuously tracked, thus obtaining image information as well as real time ground velocity information. The parameters of the limited homography were then computed as outlined in Section 3.1. We conducted 20 experiments with the actual robot and recovered the values of the homography for each case.

We compared the results that were obtained from our online calibration procedure to obtain the first 2 columns of the scaled ground plane homography, $\hat{\mathbf{g}}$, with an estimate for the ground plane homography computed from point correspondences, $\tilde{\mathbf{g}}$ - i.e. a 3×2 matrix representing the first two columns of the homography \mathbf{G} obtained from point correspondences, appropriately scaled. We defined a benchmark to judge the accuracy of the recovered parameters with regard to their values in an ideal case. Specifically, we computed the quantity, $n_e = \frac{\|\hat{\mathbf{g}} - \tilde{\mathbf{g}}\|_F}{\|\tilde{\mathbf{g}}\|_F}$.

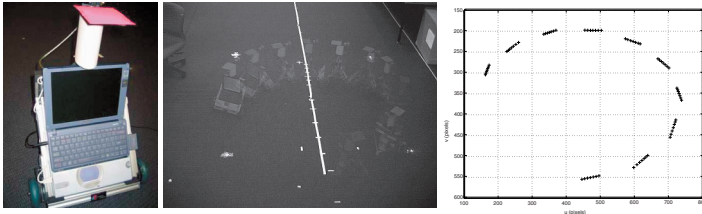


Fig. 3. The ER1 robot used for experimental runs (left) as seen by the overhead camera (center) and segments of the path traced by it (right) during a calibration run.

Over the 20 experiments tests that were conducted, the mean and median values of n_e were determined to be 0.0563 and 0.0540 respectively. A typical set of values for the recovered homography parameters as compared with the parameters recovered from point correspondences (referred to as *ideal*) are presented in Table 1.

Table 1. A Sample Comparison of Ideal and Experimental Values of the Limited Homography

$\hat{G}^1(ideal)$	$\hat{G}^1(exp)$	$\hat{G}^2(ideal)$	$\hat{G}^2(exp)$
-8.8347	-8.9873	-2.0486	-2.1911
-0.2190	-0.4488	3.3972	3.3299
-0.00064	-0.0008	-0.0048	-0.0049

5.2 Point to Point Motion of a Mobile Robot Using an Image Based Controller

During experiments that were performed in real time, the camera was first calibrated using motion correspondences and then the control scheme described in Section 4 was applied to get the robot to randomly chosen destinations in the image plane. A typical path followed by the robot is shown in Figure 4. The path taken by the robot during the calibration procedure is represented by dotted lines while the solid arcs are the path taken by the robot as it moved from one intermediate destination to another chosen in the overhead image.

5.3 Extension to a Moving Overhead Observer

So far it has been assumed that the overhead camera remained stationary during the motion of the ground vehicle. This restriction can be removed if we posit the existence of a set of 4 or more fixed points on the ground plane which can be identified and tracked over time. These point correspondences can be used to compute collineations that effectively fixate the ground plane in the image, a simple form of image stabilization. Note that we do not require any information about the inertial locations of the tracked points on the ground plane since they are only being used to compute collineations between images. This stabilization procedure returns us to the realm where the stationary camera analysis can be applied.

This procedure can be better understood by looking at the two images shown in Figure 5. These are views of the robot and the features on the ground from two

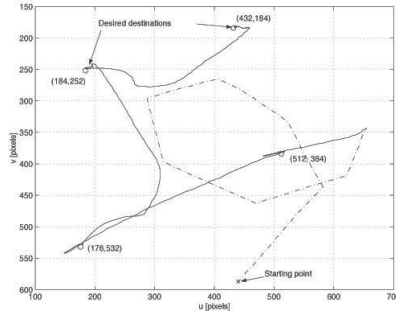


Fig. 4. The robot's path during calibration (dotted lines) and during point to point navigation (solid arcs). Intermediate destination points chosen randomly by the user are indicated by circles.

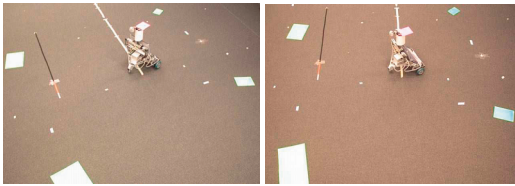


Fig. 5. The robot and fiducials as seen by the overhead camera from two viewpoints- a reference (left) and an intermediate (right) during an experiment.

different camera viewpoints, as might be seen during observations from a mobile overhead camera. Assuming that the frame on the left is the reference frame (F_{ref}) and the frame on the right is an intermediate frame, F_i , a collineation can be computed that would uniquely relate points in F_i to points in F_{ref} . Thus, at every frame, the *current* position of the robot as well as its desired destination as seen in F_i can be mapped to F_{ref} , thereby transforming the entire problem of controlling the robot to frame F_{ref} . This simple form of image stabilization has also been tested on the experimental platform in real time.

6 Conclusions

This paper considers the problem of controlling the motion of a vehicle moving on a ground plane based on the imagery acquired with an overhead camera, an important special case of the visual servoing problem. One of the primary motivations for considering this situation is the fact that overhead imagery provides a convenient context for defining motion objectives for the robot. In order to relate objectives defined in the image plane to the velocity commands passed to the vehicle we must first recover the relationship between the vehicle's velocity and the motion of its projection in the image. To this end, we propose a novel analysis of this relationship which yields some interesting insights. The analysis shows that the image velocity depends linearly upon its ground plane velocity, (\dot{x}, \dot{y}) , and quadratically upon the

location of its projection in the image, (u, v) , and a subset of the parameters of the homography relating the ground and image planes, (G^1, G^2) . More importantly, the ideas basic presented here have been implemented on a robot in 2-D experiments and we encouraged by the results which show that the schemes perform well even in the presence of measurement errors.

Our future in this area will address the development of motion and trajectory planning techniques in the image plane, and the extension to multiple uncalibrated cameras. Our ultimate goal is to be able to plan and control multiple robots in the image space.

Acknowledgment: This work was supported by NSF grants IIS02-22927 and IIS00-83240.

References

1. Ronen Basri, E. Rivlin and I. Shimshoni, "Visual Homing: surfing on the epipoles", *International Conference on Computer Vision, 1998*.
2. W.E. Dixon, D.M. Dawson, E. Zergeroglu, and A. Behal, "Adaptive tracking control of a wheeled mobile robot via an uncalibrated camera system", *SMC-B*, 31(3):341—352, June 2001.
3. Gregory D. Hager, "Calibration-free visual control using projective invariance". In *Proc. IEEE Conf. on Comp. Vision and Patt. Recog.*, pages 1009—1015, 1995.
4. Nicholas Hollinghurst and Roberto Cipolla, "Uncalibrated stereo hand-eye coordination". *Image and Vision Computing*, 12(3):187—192, April 1994.
5. S. Soatto and P. Perona, "Structure-independent visual motion control on the essential manifold". In *Proc. of the IFAC Symposium on Robot Control (SYROCO)*, Capri, Italy, pages 869—876, Sept 1994.
6. G. S. Hornby and S. Takamura and J. Yokono and O. Hanagata and T. Yamamoto and M. Fujita, "Evolving Robust Gaits with AIBO", In *Proc. 2000 Int. Conf. Robotics and Automation*, San Francisco, CA, pages 3040- 3045.
7. C. J. Taylor, J. P. Ostrowski and Sang Hack Jung, "Robust Visual Servoing based on Relative Orientation", In *Proc. IEEE Conf. on Computer Vision and Pattern Recognition*, Fort Collins, CO, pages 574-580.
8. Hong Zhang and James P. Ostrowski, "Visual servoing with dynamics: Control of an unmanned blimp", In *Proc. IEEE Int. Conf. Robotics and Automation*, 1999, Detroit, MI, pages 618- 623.
9. Yi Ma, Jana Košecá and Shankar Sastry, "Vision guided navigation for a nonholonomic mobile robot", *IEEE Trans. on Robotics and Automation*, 1999, 15(3), pages 521-536.
10. Gideon P. Stein, Ofer Mano and Amnon Shashua, "A Robust Method for Computing Vehicle Ego-motion", In *IEEE Intelligent Vehicles Symposium (IV2000)*, Dearborn, MI.
11. S. Hutchinson, G. Hager and P. Corke, "A Tutorial on Visual Servo Control", *IEEE Trans. on Robotics and Automation*, May 1996.
12. Ezio Malis, François Chaumette and Sylvia Boudet, "2 1/2 D Visual Servoing", *IEEE Trans. on Robotics and Automation*, 1999, 15(2), pages 238-250.
13. N. J. Cowan and D. E. Koditschek, "Planar image based visual servoing as a navigation problem", In *Proc. IEEE Int. Conf. Robotics and Automation*, 1999, pages 611-617.
14. Ben Grocholsky, Selcuk Bayraktar, Vijay Kumar, Camillo J. Taylor and George Pappas, "Synergies in Feature Localization by Air-Ground Robot Teams", *International Symposium on Experimental Robotics*, Singapore, June 2004.